Historical black carbon deposition in the Canadian High Arctic: A 190-year long ice-core record from Devon Island

Christian M. Zdanowicz[1], Bernadette C. Proemse[2], Ross Edwards[3], Wang Feiteng[3,4], Chad M. Hogan[2], Christophe Kinnard[5].

[1]Department of Earth Sciences, Uppsala University, Uppsala, 75646, Sweden
[2]School of Biological Sciences, University of Tasmania, Hobart, TAS7001, Australia
[3]Physics and Astronomy, Curtin University, Perth, WA6102, Australia
[4]Cold and Arid Regions Environment and Engineering Research Institute, Chinese Academy of Sciences, Lanzhou, China
[5]Département des Sciences de l'Environnement, Université du Québec à Trois-Rivières, Trois-Rivières, G9A 5H7, Canada

Correspondence to: Christian M. Zdanowicz (christian.zdanowicz@geo.uu.se)

Abstract. Black carbon aerosol (BC) emitted from natural and anthropogenic sources (e.g., wildfires, coal burning) can contribute to magnify climate warming at high latitudes by darkening snow- and ice-covered surfaces, thus lowering their albedo. Modeling the atmospheric transport and deposition of BC to the Arctic is therefore important, and historical archives of BC accumulation in polar ice can help to validate such modeling efforts. Here we present a 190-year ice-core record of refractory BC (rBC) deposition on Devon ice cap, Canada, spanning calendar years 1810-1990, the first such record ever developed from the Canadian Arctic. The estimated mean deposition flux of rBC on Devon ice cap for 1963-1990 is 0.2 mg m^{-2} a^{-1}, which is low compared to most Greenland ice-core sites over the same period. The Devon ice cap rBC record also differs from existing Greenland records in that it shows no evidence of a substantial increase in rBC deposition during the early-mid 20th century, which, for Greenland, has been attributed to mid-latitude coal burning emissions. The deposition of other contaminants such as sulfate and Pb increased on Devon ice cap in the 20th century but without a concomitant rise in rBC. Part of the difference with Greenland may be due to local factors such as wind scouring of winter snow at the coring site on Devon ice cap. Air back-trajectory analyses also suggest that Devon ice cap receives BC from more distant North American and Eurasian sources than Greenland, and aerosol mixing and removal during long-range transport over the Arctic Ocean likely masks some of the specific BC source-receptor relationships. Findings from this study underscore the large variability in BC aerosol deposition across the Arctic region that may arise from different transport patterns. This variability needs to be accounted for when estimating the large-scale albedo lowering effect of BC deposition on Arctic snow/ice.

1 Introduction

The deposition of light-absorbing carbonaceous particles emitted by the incomplete combustion of biomass and fossil fuel can decrease the albedo of Arctic snow- and ice-covered surfaces, thereby amplifying high-latitude warming driven by the buildup of greenhouse gas emissions (AMAP, 2011; Bond et al., 2013). The widely used expression "black carbon" (BC) designates the insoluble, refractory fraction of these aerosols that is largely made of graphitic elemental carbon and strongly

Atmospheric
Chemistry
and Physics
Discussions

absorbs light at visible to near-infrared wavelengths (Petzold et al., 2013). Along with sulfate (SO_4^{2-}), BC is one of the main short-lived climate pollutants being targeted for mitigation and control under multinational legal agreements (Quinn et al., 2008; AMAP, 2015).

In order to evaluate how past and future BC emissions have affected, and will affect, climate forcing in the Arctic,
5   global atmospheric/climate models can be used to simulate the transport and deposition of BC aerosols in this region (Koch et al., 2011; Lee et al., 2013; Jiao and Flanner, 2016). At present, simulated BC dispersion suffers from large biases, either positive or negative, compared with observational data on BC in Arctic air and snow (Jiao et al., 2014). Validating model simulations is difficult because of the scarcity of such observations across the Arctic. Direct monitoring of atmospheric BC is so far limited to a few decades and at a few stations (Hirdman et al., 2010; Gong et al., 2010), and geographic surveys of
10 BC in snow and ice are rare and difficult to conduct over the vast Arctic region (e.g., Doherty et al., 2010).

Ice cores drilled from the accumulation area of glaciers and ice caps can be used as surrogates for direct atmospheric observations, as they contain archives of BC and other aerosol species deposited in snow over many centuries (McConnell, 2010). At present, ice-core records of BC deposition in the Arctic region are only available from Greenland (McConnell et al., 2007, McConnell and Edwards, 2008; Koch et al., 2011; Lee et al., 2013) and from Svalbard (Ruppel et
15 al., 2014). Here, for the first time, we present a historical record of BC deposition in the Canadian Arctic, developed from a core drilled on Devon Island ice cap, and spanning the years ~1810-1990. The Devon ice cap BC record presents striking differences from Greenland records. We discuss the possible reasons for these differences, and consider the implications with respect to regional BC transport and deposition patterns in the Arctic region.

2 Study site

20 At latitude 75° N, Devon ice cap (14,400 km^2) occupies a central position in the eastern Canadian Arctic Archipelago and lies 275 km from the Greenland coast across northern Baffin Bay. The ice cap has been studied for half a century (Boon et al., 2010) and was previously drilled to obtain records of climate and atmospheric contaminants (e.g., Goto-Azuma and Koerner 2001; Shotik et al., 2005; Kinnard et al., 2006). However, no record of BC deposition was ever developed from this or any other site in the Canadian Arctic. The core used in the present study (DV99.1) was obtained in April 1999 by the
25 Geological Survey of Canada (GSC) at a site (75.32° N, 81.64° W, 1750 m.a.s.l) located 25 km to the east of the ice cap's true summit (1930 m.a.s.l) (**Fig. 1**). The coring site lies above the present-day equilibrium-line altitude (ELA) which is >1500 m a.s.l on this part of Devon ice cap, and has an estimated mean net accumulation rate ($\dot{A}$) of 0.14 m a^{-1} water equivalent (see below).

Atmospheric
Chemistry
and Physics
Discussions

3 Materials and methods

3.1 Core sampling and analyses

Few measurements were conducted on the DV99.1 core prior to this study. At the time of coring, the solid-state DC electrical conductivity (EC) of the ice was measured continuously at mm-scale resolution using parallel electrodes, as

5   described in Zheng et al. (1998). Subsequently, the core was sampled at 5- to 20-cm resolution for the determination of stable oxygen isotope ratios ($\delta^{18}O$) by mass spectrometry at the University of Copenhagen. The remaining half-cores were stored frozen (-20°C) inside sealed polyethylene bags at the GSC ice-core laboratory, until archived core segments between 4 and 38 m depths were selected for this study and shipped, still frozen, to Curtin University in Australia for BC analyses. These combined core segments were initially estimated to span ~200-250 years, as explained below. The uppermost 4 m of

10   the firn core were not sufficiently consolidated to be usable, and were discarded. Core segments below ~40 m were micro-fractured during drilling, and were also unsuitable for analysis.

Sample preparation and analysis was conducted at the Advanced Ultra-clean Environment Facility at Curtin University (class 100). The DV99.1 core sections (~1 m each in length) were cut into sticks with a ~2.5 × 2.5 cm cross-section, which were processed in an ice-core melter coupled to a Continuous Flow Analysis (CFA) system. The meltwater was aerosolized

15   with a U5000AT ultrasonic nebulizer (CETAC Technologies, Omaha, NE, USA) and injected into a single-particle intracavity laser-induced incandescence photometer (SP2, Droplet Measurement Technologies, Boulder, CO), which measured the mass concentration of BC particles in the meltwater flow (Bisiaux et al., 2012; McConnell et al., 2007, McConnell and Edwards, 2008). Following Petzold et al. (2013), we refer to the BC fraction measured by this method as *refractory BC*, abbreviated rBC, reported here in mass concentration units of ng g^{-1}. In addition to rBC, insoluble

20   microparticles with diameters between 0.9 and 15 µm were quantified in the meltwater flow using an inline Abakus laser particle counter (Markus Klotz GmbH, Bad Liebenzell, Germany), as described elsewhere (Ruth et al., 2003). The recorded microparticle counts per second were converted to number of particles per milliliter of meltwater (part. mL^{-1}) by taking into account the effect of firn densification and annual layer thinning with depth in the DV99.1 core.

To compare the DV99.1 record of rBC and microparticles with that of other aerosol species, we used

25   glaciochemical data obtained from two other cores drilled from the summit of Devon ice in 1998 (core DV98.3) and in 2000 (core DV2000) (Fig. 1). The DV98.3 core was sampled continuously and analyzed for eight major ionic species by ion chromatography, as described in Kinnard et al. (2006). In this study, we used SO_4^{2-}, sodium (Na$^+$), calcium (Ca^{2+}), potassium (K$^+$) and ammonium (NH$_4^+$) data obtained from the top 85 m of the core, which had been sampled at 3- to 12-cm resolution. The non-sea salt (nss) fraction of SO_4^2 and Ca^{2+} was estimated from Na^{2+} using the mean surface seawater composition of

30   Pilson (2012), and the biomass burning fraction (BB) of K$^+$ was estimated from Na^{2+} and Ca^{2+} following Legrand et al. (2016). The DV2000 core was drilled at the same site as the DV98.3 core, and was analyzed for lead (Pb) and other trace metals by sector field inductively coupled mass spectrometry, as reported in Shotyk et al. (2005). The remaining archived

Atmospheric
Chemistry
and Physics
Discussions

volume from cores DV98.3 and DV2000 was, however, insufficient to carry out rBC analyses, which is why core DV99.1 was used for this purpose.

3.2 Age models

Annual layers are not easily resolved in cores from Canadian Arctic ice caps, partly owing to relatively low $\dot{A}$, but also to the effects of wind and/or summer surface melt. Therefore, age models developed for these cores are commonly based on a variety of alternative methods. For the DV98.3 and DV99.1 cores, an ice-flow model approximation (Dansgaard and Johnsen, 1969) was used, constrained by the total ice thickness obtained from ice-radar measurements or from borehole depths, and by the estimated $\dot{A}$ at each coring site. For the DV98.1 core, the preliminary age model was refined by approximate layer counting using glaciochemical data at shallow depths, and, at greater depths, from the identification of fallout of radionuclides from surface nuclear bomb tests (1963) and of acidic aerosols (H_2SO_4) from dated historical volcanic eruptions, including that of Laki, Iceland, in 1783, which is the largest and most recognizable historical volcanic signal recorded in Canadian Arctic ice caps (Fisher and Koerner, 1994; Zheng et al., 1998; Kinnard et al., 2006).

The DV99.1 core does not have well-preserved annual glaciochemical or isotopic ($\delta^{18}O$) signals that could be reliably used for layer counting. Hence, the age model developed for this core is primarily based on an ice-flow model approximation. For the uppermost ~45 m, a reference horizon was provided by a large EC (acidity) spike at a depth of 42.60 m (29.56 m ice equivalent), attributed to fallout from the 1783 Laki eruption. Using this marker, the estimated value of $\dot{A}$ at the DV99.1 site is 0.14 m a^{-1}, which is lower than at the ice cap summit (0.23 m a^{-1}) or at sites elsewhere in the accumulation zone (0.17-0.25 m a^{-1}; Colgan and Sharp, 2008). The most likely explanation is partial scouring of winter snow layers by downslope winds at the DV99.1 site, as also observed on parts of Agassiz ice cap (Fisher et al., 1983). This is supported by a comparison of $\delta^{18}O$ variations measured in the DV99.1 core with those in core DV98.3, which shows that $\delta^{18}O$ variations in the DV99.1 core are truncated of their most negative ("coldest") values relative to the DV98.1 core (Supplement: **Fig. S1**). An estimate of the amount of snow lost by wind scouring at the DV99.1 site can be made from the $\delta^{18}O$ data, following Fisher and Koerner (1988). The calculation suggests that ~40-45 % of the annual snow accumulation is removed by wind at this site, compared to the summit of Devon ice cap. Based on this assumption, the predicted age of the Laki 1783 volcanic signal is approximately 29 m (ice equivalent), and this agrees closely with the depth of the observed EC peak attributed to the eruption (29.56 m).

The adopted depth-age models for the DV98.3 core (TIME4.D98) and the DV99.1 core (TIME3.D99) are presented on **Fig. 2**. The DV2000 core was drilled at the DV98.3 coring site and used the same age model. Down to the Laki volcanic marker, the age models for the DV98.3 and DV99.1 cores are both nearly linear with respect to ice-equivalent depth. Based on the TIME3.D99 age model, the rBC and microparticle records developed from the DV99.1 core are estimated to span calendar years 1810-1990. Analyses for rBC and microparticles were both performed at mm-scale resolution along the core. The data were subsequently averaged over discrete depth increments approximately equivalent to 1- and 10-year intervals,

respectively. In this paper, annually-averaged figures are used for illustrative purposes only, as discrete, accurate ages can not be confidently ascribed to these data (see below).

3.3 Quantifying uncertainties in the ice core record

Down-core variations of atmospheric impurities (such as rBC) in firn and ice cores are the result of a combination of processes, including temporal changes in net atmospheric deposition rates (fluxes, abbreviated F), stochastic spatial variations of deposition of the aerosols in snow (ε_s), and post-depositional modifications (e.g., by wind scouring), to which are added uncertainties arising from potential errors in the age model (ε_t). To determine if measured down-core variations in impurities result from changes in F requires ε_s and ε_t, as well as the effects of post-depositional changes, to be estimated.

Uncertainties in the assigned age of firn or ice layers between horizons of assumed or known age can arise due to interannual variations in $\dot{A}$. In order to estimate these errors in the DV98.3 and DV99.1 records, we used a Monte Carlo simulation implemented in Matlab™ ($N = 1000$ realizations). Briefly, the script uses a constrained random walk algorithm to estimate the probabilistic distribution of the true age at any depth between reference layers of known age (Kinnard et al., 2006). For both the DV98.3 and DV99.1 cores, these reference layers were the surface and the Laki volcanic horizon (1783). In the Monte Carlo simulation, interannual variations in $\dot{A}$ are considered to behave as a stationary, autoregressive blue noise process with a lag-one serial autocorrelation coefficient of -0.5 to -0.3, following Fisher et al. (1985). For each realization of the simulation, a new age model is generated, and the cumulative probabilistic error ε_t on firn age estimates is computed for all depths between the reference horizons. One- and 10-year averages of the ice core glaciochemical data were also computed separately for each age model iteration, in order to estimate the spread in results caused by ε_t.

The spatial variability of atmospheric deposition in snow for aerosol species such as ions, rBC or microparticles has never been directly measured on Canadian Arctic ice caps. However for Devon ice cap, it can be calculated or estimated from major ion analyses performed on an array of shallow cores (Colgan and Sharp, 2008; **Fig. 1**). The coefficient of spatial variation for annual net deposition of SO_4^{2-} was estimated to be ~42 %. Here, we make the assumption that atmospheric deposition of rBC and insoluble particles on Devon ice cap share the same spatial variability as SO_4^{2-}, an aerosol species which, like BC but unlike others such as nitrate (NO_3^-), is not subject to re-emission from snow to air. These estimates of ε_s were used to generate white Gaussian noise, which was then added to the ice core data as part of the Monte Carlo procedure described above, thus integrating in the simulation the effects of spatial variability in aerosol deposition over the ice cap. Because the magnitude of ε_s is independent from that of errors that arise from ice core dating uncertainties (ε_t), the combined uncertainty was calculated as the quadratic sum of these terms ($\pm 2\sigma$). The possible effects of post-depositional processes, such as wind scouring or meltwater percolation, are discussed below.

4 Results and discussion

4.1 The DV99.1 record of rBC and microparticle deposition

Depth profiles of rBC and microparticles measured in the DV99.1 core are shown in **Fig. 3**. Both parameters have probability distributions which are approximately log-normal (**Fig. S2**), and we therefore use both the arithmetic and geometric means (μ, μ_g), as descriptive metrics for these data. Over the length of core analyzed, rBC concentrations average 1.5 ± 3.2 ng g^{-1} ($\mu_g = 0.9$ ng g^{-1}) with a maximum of 74 ng g^{-1}, and microparticle concentrations average $500 \pm 496 \times 10^3$ part. mL^{-1} ($\mu_g = 395 \times 10^3$ part. mL^{-1}) with a maximum of 5637×10^3 part. mL^{-1}. The mean rBC concentration remains approximately constant between ~38 and 15 m depths, and decreases gradually at shallower depths to reach ~1.0 ng g^{-1} ($\mu_g = 0.5$ ng g^{-1}) in the uppermost 1-m core section analyzed. In contrast, microparticle concentrations are higher above ~15 m depth, averaging 606×10^3 part. mL^{-1} ($\mu_g = 376 \times 10^3$ part. mL^{-1}), compared to 462×10^3 part. mL^{-1} (geom. mean 325×10^3 part. mL^{-1}) below 15 m. Through the entire core, most microparticles (98 %) are < 5 μm in size, with no significant variations in the contribution of larger particles (5-15 μm). The observed changes in rBC and microparticle concentrations near 15 m depth do not correspond to any clear step change in the physical stratigraphy or density in core DV99.1 (**Fig. 3**).

Reconstructed variations in aerosol deposition from ice cores spanning calendar years 1800-1990 (**Fig. 4**) show that Devon ice cap experienced an increase in atmospheric deposition of Pb and nssSO$_4^{2-}$ during the 20th century, consistent with trends in mid-latitude anthropogenic emissions from fossil fuel combustion (Lamarque et al., 2010). Microparticle concentrations in the DV99.1 also rose in the early 20th century and remained elevated thereafter, which suggests that the rise was associated to that of anthropogenic pollution. Relative to Na$^+$, concentrations of Ca^{2+} and K$^+$ in the DV98.3 core are far in excess of those in surface seawater, indicating these ionic species are predominantly from non-marine sources, for e.g., mineral dust. However, there are no large enhancements in nssCa^{2+} and nssK$^+$ in the DV98.3 core corresponding to the increase in microparticle deposition seen in the DV99.1 core during the 20th century (**Fig. 4**; only nssCa^{2+} is shown), indicating that the latter increase was unrelated to change in atmospheric dust inputs.

There is also no large or sustained increase in rBC deposition in the DV99.1 core during the 20th century concomitant with that of nssSO$_4^{2-}$, Pb or microparticles. This contrasts with ice-core records from Greenland, which show noticeably large increases of both rBC and non-salt sulfur (nssS) in the early 20th century, although the relative timing and magnitude of these increases differ between core sites (**Fig. 5** and **6**). In Greenland cores, rBC deposition peaked in the 1910s-20s, and decreased thereafter (McConnell et al., 2007; Koch et al., 2011), in step with historical changes in coal BC emissions from the USA and Europe (Novakov et al., 2003; Bond et al., 2007; Skeie et al., 2011). At the ACT2 site (66° N), the early 20th century rise in rBC and nssS was also accompanied by increased deposition of Pb and other trace metals (McConnell and Edwards, 2008). The highest rBC concentrations in the DV99.1 core also occur in the decade 1910-1920 ($\mu = 3.6$ ng g^{-1}, $\mu_g = 1.6$ ng g^{-1}) and decrease thereafter, but the magnitude and duration of this early 20th period of enhanced rBC deposition are much less than in Greenland cores. These differences are somewhat surprising, given the relative

proximity of Devon ice cap from Greenland. In order to explain our findings, both site-specific and regional-scale factors must be considered.

4.2. Site-specific factors

Observations of atmospheric BC at Alert on Ellesmere Island (82° N, see **Fig. 1** for location) show a seasonal cycle with airborne concentrations peaking during winter and spring months (December-March) and declining to their minimum in summer and early autumn months (June-September) (Gong et al., 2010). Most BC deposition in snow is thought to occur in spring and summer, when increased cloudiness promotes in-cloud scavenging and wet deposition of the hydrophilic fraction of BC (Browse et al., 2012; Shen et al., 2017). In the interior of the Greenland ice sheet, the seasonal cycle of BC deposition is well-preserved in snow and firn layers (e.g., McConnell et al., 2007). This is not the case at the DV99.1 core site on Devon Island. Even in the uppermost part of the core, where some seasonal $\delta^{18}O$ variations can be detected, there is no recognizable seasonal pattern of rBC concentration peaks (**Fig. S3**). This is likely the result of the combined effects of wind scouring/mixing of surface snow (as described earlier) and of summer surface melt. It is therefore legitimate to ask whether these processes could also have obliterated or masked a 20th century anthropogenic signal in the DV99.1 rBC record.

The seasonally-resolved ice core record from site D4 in Greenland (71°N; see **Fig. 1** for location) shows that during the historical period of enhanced anthropogenic BC pollution in the Arctic, from the late 19th to mid 20th centuries, rBC deposition increased in both summer and winter (McConnell et al., 2007). If the Canadian High Arctic was impacted by airborne BC pollution in a similar way, one would expect to find a marked increase in rBC concentrations in the DV99.1 core during the late 19th to mid 20th centuries, even if winter snow layers were scoured away by wind. To verify this, we performed a simple simulation in which we generated synthetic time series of rBC deposition spanning the period 1810-1990, with a seasonal cycle superimposed on baseline interdecadal variations similar to those observed in the Greenland D4 ice-core record. Winter rBC deposition peaks in the series were represented using a log-Gaussian function, and their amplitude was allowed to vary from year to year to produce a range of temporal variations comparable to, or lower than, that seen in the Greenland D4 core. Winter deposition peaks were then randomly truncated by 30-60 % to simulate the effects of wind scouring on the record, and 5-year running means were computed from the resulting data, the smoothing being used to simulate the possible effects of post-depositional snow layer mixing by wind. Results of these experiments showed that even if the wintertime rBC deposition peaks between November to May were largely truncated by wind, the low-frequency baseline variation would still persist, and should be recognizable above the remaining interannual signal variance (**Fig. 7**). It therefore seems unlikely that wind scouring alone would completely obliterate this signal in the DV99.1 record, not unless the amplitude of the seasonal cycle of atmospheric BC deposition on Devon ice cap is much lower than observed at Alert or in Greenland (Gong et al., 2010; Massling et al., 2015).

Unlike much of central Greenland, the summit of Devon ice cap is also regularly subject to partial melting at the surface during summer months, and meltwater can percolate and refreeze into the underlying snow and firn to form infiltration ice features, or, more simply, "melt layers". The volumetric percentage of melt layers in core DV99.1 was

measured by Fisher et al. (2012) as a proxy for past summer warmth. They found that surface melt rates increased abruptly in the mid-19th century following the end of the Little Ice Age cold interval, and have since varied between ~40 and 60 % (average) per 5-year period, with an interval of noticeably lower melt rates (down to 10 %) between ~1880 and 1930 (**Fig. 4**). One must therefore consider whether surface melt could account for the apparent limited baseline variability in the DV99.1 rBC record during the 19th and 20th centuries.

5

The post-depositional mobility of BC particles in melting snow is not well known, and likely depends on the hydrophobicity of these particles, which is largely influenced by the presence or absence of surface coatings, for e.g., with SO_4^{2-} (Liu et al., 2011, Liu et al., 2013). Doherty et al. (2013) investigated the vertical redistribution of BC and other light-absorbing particles in snow and firn near Dye 2 (66° N; ~2100 m a.s.l.; see **Fig. 1** for location) in a part of the Greenland ice sheet's percolation zone where melt layers up to 20 cm thick are now commonly found (de la Peña et al., 2015; Machguth et al., 2016). Only a very limited amount of vertical redistribution of BC was observed in the snow and firn, and surface melt and percolation did not obliterate seasonal variations of BC in the firn stratigraphy. Doherty et al. (2013) attributed this result to the low scavenging efficiency of these particles by meltwater (~20-30 %). At the DV99.1 site on Devon Island, $\dot{A}$ (0.14 m a^{-1}) is only half of that in the Dye 2 area (~0.32 m a^{-1}; Buchardt et al., 2012), and surface melt there could mask some seasonal variations of rBC in the firn. However, the findings of Doherty et al. (2013) suggest that this should not be sufficient to mask or completely smooth out down-core variations in rBC concentrations when these are averaged over decadal intervals.

10

15

There is, however, another consideration. Unlike in the Doherty et al. (2013) study, rBC concentrations in the DV99.1 core were measured by SP2, and the detection efficiency of this method for BC in liquid samples depends on the type of nebulizer used for inflow. Schwarz et al. (2012) and Wendl et al. (2014) have shown that the relative areosolization efficiency of the U5000AT ultrasonic nebulizer used in the analysis of the DV99.1 core drops rapidly at or below 10 % for particles with a volume-equivalent diameter ≥ ~600 nm. Given that coagulation and agglomeration is known to increase the size of BC particles during thaw and refreezing of snow (Schwarz et al., 2013), this raises the possibility that the SP2 may have underestimated the true mass concentration of BC particles in that part of the DV99.1 core corresponding to the 20th century, since this period has been characterized by high rates of melt layer formation in firn at the coring site (**Fig. 4h**). The Greenland sites from which ice-core rBC records were developed by the SP2 method (**Fig. 5**) are comparatively less affected by surface melt and ice layer formation than Devon ice cap, and BC particles in firn at these sites may therefore undergo lesser post-depositional coagulation. Whether this effect alone could explain the lack of baseline variability in the DV99.1 rBC record seems unlikely, but it could have contributed to mask some of the variations in atmospheric BC deposition in the core, and it might account for the apparent discrepancy between trends in rBC and microparticle deposition during the 20th century (**Fig. 4c,d**), if the former are more efficiently detected than the latter.

20

25

30

Atmospheric
Chemistry
and Physics
Discussions

4.3 Regional-scale factors

Other reasons for the contrast between the DV99.1 and Greenland rBC records (**Fig. 5** and **6**) may be found in the atmospheric transport paths that deliver BC to the Canadian High Arctic, relative to Greenland. Shindell et al. (2008) used multiple atmospheric transport models to investigate the sensitivity of near-surface airborne BC concentrations in the Arctic to regional anthropogenic emissions. They found that Europe and North America likely contribute equally to BC deposition over Greenland, whereas the central and Russian sectors of the Arctic are predominantly affected by European emissions. Atmospheric BC in the Canadian High Arctic may be affected by both European and North American emissions, but is expected to be much less sensitive to changes in these emissions compared to other parts of the Arctic, partly because it is very remote from all BC source regions (Shindell et al., 2008; their Fig. 9 and 10).

Sharma et al. (2006) and Huang et al. (2010) used air back-trajectory analyses to investigate the probable source regions of BC detected in surface air at Alert in winter and spring, and identified Russia and Europe as dominant, followed by North America. The summit of Devon ice cap is 1000 km further south and ~1.8 km higher, and could thus be affected by a different mix of BC source contributions than Alert. To verify this, and also to contrast the situations of Devon ice cap and Greenland, we computed ensemble 10-day air back-trajectories from both Devon ice cap summit and from Summit, Greenland, using the HYbrid Single-Particle Lagrangian Integrated Trajectory model (HYSPLIT v.4) of the NOAA Air Resources Laboratory (Draxler and Hess, 2014, Stein et al., 2015). As input, we used meteorological fields of the NCEP-NCAR 50-year reanalysis product, which are available on a global $2.5 \times 2.5°$ grid at 6-hourly temporal resolution (Kistler et al., 2001). Back-trajectories starting daily at 12:00 PM UTC were computed over the period 1948-1999. Unlike Sharma et al. (2006) and Huang et al. (2010), however, we did not use trajectory clustering, because results are highly sensitive to the quality and density of meteorological data coverage used in trajectory computations, and to the arrival height of trajectories (i.e., starting point of back-trajectories; Kassomenos et al., 2010; Su et al., 2015). Instead, we computed probability density maps or air parcel residence time from all combined trajectories over an equal area grid with 200×200 km resolution, following a methodology analog to that of Miller et al. (2002).

Results (**Fig. 8**) show that for 10-day transport periods, air parcels arriving at Greenland Summit are more commonly advected from the south-southwest than from other cardinal directions, and frequently reach central Greenland after transiting over the North Atlantic, consistent with earlier findings by McConnell et al. (2007; Their Fig. S1). In contrast, air that reaches the summit of Devon ice cap comes more frequently from the west-northwest, and transits over the Arctic Ocean, which agrees with findings from analyses of low-level air transport to Devon ice cap by Colgan and Sharp (2008) for the period 1979-2003. It is therefore likely that a large part of BC transported to Devon ice cap is from regional emission sources located in northwestern North America and/or in the central or eastern parts of Eurasia.

Smoke plumes from forest or grassland fires, natural or provoked, can reach the Arctic and contribute to BC pollution, particularly during summer (Stohl et al., 2006; Paris et al., 2009; Warnecke et al., 2009; Quennehen et al., 2012; Zennaro et al., 2014). Back-trajectory analyses of BB aerosols detected at Eureka on Ellesmere Island (80° N; **Fig. 1**)

indicate, unsurprisingly, that boreal forest/grassland regions of Russia and Canada are the dominant source regions for these long-range plume transport events, followed by north-central USA and Alaska, (Viatte et al., 2015). To evaluate the impact of forest/grassland fire emissions on BC deposition to Devon ice cap, we compared the DV99.1 rBC record with reconstructed historical variations in fire frequency and/or burned area across Canada and Russia during the 19th and/or 20th

5   centuries (**Fig. 9**). On an interdecadal time scale, no statistically meaningful correlations ($p < 0.05$) were found between the DV99.1 rBC record and fire histories from Canada (Girardin, 2007; Girardin and Sauchyn, 2008; Girardin et al., 2006). If wildfires in northern Canada contribute to rBC deposition on Devon ice cap, these contributions do not appear to covary in any simple way with variations in fire frequency or burned area. However, the decrease in rBC deposition recorded in the DV99.1 core after the 1910s is concomitant with a general decrease in fire frequency in the boreal forests of Russia that

10   continued until the 1980s, and which was due to fire suppression measures and land use changes in these regions (Mouillot and Field, 2005).

To investigate this finding more closely, we regressed the decadally-averaged DV99.1 record of rBC deposition against gridded (0.5 x 0.5°) maps of historical decadal mean BC emissions from BB sources (forest/grassland fires) compiled by Lamarque et al. (2010) and covering the period 1890-1990 (**Fig. 10**). We did not perform this analysis for anthropogenic

15   BC emissions because geographical inconsistencies in the gridded emission data resulted in correlation artefacts. For most of the 20th century, the data on BB emissions from Russia and central Asia are largely based on the historical fire inventory of Mouillot and Field (2005). The only geographic area where strong ($R > 0.5$) positive correlations were found with the DV99.1 rBC record corresponds with a broad sector between 45-55°N, and 30-90°E, at the southern fringe of the Russian boreal forest belt and the steppe/grasslands of Kazakhstan. These regions are particularly fire-prone, and have been identified

20   as important sources of CO and of BC aerosols transported over Siberia and into the Arctic atmosphere (Vasileva et al., 2011, Cheng, 2014, Rault et al., 2017). The spatial pattern of correlations on **Fig. 10** suggests that forest/grassland fires across south-central Russia and Kazakhstan contribute more to the long-range transport of BC aerosols to the Canadian High Arctic than wildfires in the North American boreal forest belt. However, only some parts of the area of interest have R values that pass a test of field significance at the 10% level of confidence (Wilks, 2016; Benjamini and Yekutieli, 2001). This is

25   unsurprising, considering the uncertainties inherent to the DV99.1 rBC record (§ section 3.3) and to the fire inventories used for the gridded BC emission maps (Mouillot and Field, 2005).

Aerosol species such as K^+ or NH_4^+ are commonly associated with BB emissions, and as such are often used as BB tracers in polar snow (Simoneit, 2002; Legrand et al., 2016). Cheng (2014) identified sectors of south-central Russia and Kazakhstan as source regions for both BC and K^+ aerosols transported to Alert between 2000 and 2002. However, we did not

30   find any significant correlations ($p > 0.05$) between interdecadal variations of rBC in the DV99.1 core and either $(K^+)_{BB}$ or NH_4^+ in the DV98.3 record (**Fig. 4f,g**). Whatever contributions BB emissions make to $(K^+)_{BB}$ or NH_4^+ deposition on Devon ice cap, these do not covary directly with rBC deposition, possibly due to mixing from multiple emission sources. For example, ammonia (NH_3) emissions from seabird colonies near Baffin Bay may be a larger regional source of NH_4^+ to Devon ice cap than distant wildfires (Wentworth et al., 2016).

4.4 Atmospheric BC deposition rates

In 90 % of the analyzed DV99.1 core, rBC concentrations are < 3 ng g^{-1}, and in the uppermost section of the core (depths 3-4 m), they are mostly < 1 ng g^{-1}. These numbers are low compared with estimated median BC concentrations of 8-14 ng g^{-1} reported by Doherty et al. (2010) for seasonal snow sampled across the Canadian Arctic in 2009. Such a large difference is

5   surprising, given that atmospheric monitoring at Alert has shown a continuous decrease in airborne BC levels since 1989 (Hirdman et al., 2010). One would therefore expect higher, not lower, rBC concentrations in snow that accumulated in the 1980s, relative to 2009. Part of the apparent discrepancy may be due to differences in analytical methods: The estimated BC concentrations in snow reported by Doherty et al. (2010) are based on a spectrophotometric technique which tends to yield larger mass concentrations relative to the SP2 method (Schwarz et al., 2012). Also, as stated earlier, rBC levels measured in

10   the DV99.1 core may underestimate actual deposition due to wind scouring of winter snow, or to inadequate aerosolization of some rBC by the ultrasonic nebulizer. It is also likely that atmospheric BC deposition over the summit region of Devon ice cap is lower than near sea level, where most of Doherty et al.'s (2010) snow samples were obtained, because the ice cap's accumulation area (≥ ~1500 m a.s.l.) is above the typical altitude range of low-level Arctic stratocumulus cloud decks which promote aerosol scavenging (Browse et al., 2012).

15   We estimated the late 20th century mean atmospheric flux of rBC (F_{rBC}) over the summit region of Devon ice cap using measurements of rBC concentrations in the DV99.1 core for 1963-1990, and data on spatial and temporal variations of $\dot{A}$ from Colgan and Sharp (2008) and from winter mass balance surveys carried out over the ice cap since the early 1960s (Fisher et al., 2012). The period 1963-1990 was selected because the 1963 radioactive layer found in Devon ice cap firn provides a firm reference level to constrain estimates of $\dot{A}$ (Colgan and Sharp, 2008). Our calculations yield a mean F_{rBC} of

20   0.2 ± 0.1 mg m^{-2} a^{-1}. If μg, rather than μ, is used as an estimate of average rBC concentrations, the estimated F_{rBC} is only slightly lower (0.1 mg m^{-2} a^{-1}). And if the annual mean concentration of rBC is assumed to be underestimated by 20-40 % due to selective wind scouring of winter snow layers, the adjusted figures for F_{rBC} are only slightly higher, ranging from 0.2 to 0.3 mg m^{-2} a^{-1} .

       These estimates are at the low end of calculated F_{rBC} in Greenland cores over the same period, which vary from

25   ~0.1 to ~4 mg m^{-2} a^{-1} (Lee et al., 2013). They are also much lower than historical fluxes of EC in the Norwegian Arctic inferred from a Svalbard ice core, which range from ~3 to nearly 40 mg m^{-2} a^{-1} between 1960 and 2004 (Ruppel et al., 2014; see **Fig. 5** for location). Overall, rBC or EC concentrations in Arctic firn and ice cores increase with mean $\dot{A}$ (**Fig. S4**), likely reflecting the amount of precipitation scavenging in different geographic sectors (Garrett et al., 2011; Browse et al., 2012). The remarkably low F_{rBC} at the DV99.1 site is probably due, at least in part, to the very low $\dot{A}$ on Devon ice cap (0.14-0.25

30   m a^{-1}; Colgan and Sharp, 2008), notwithstanding the added effects of wind scouring. However, it is noteworthy that between 1960 and 1990, the estimated F_{rBC} at the Humboldt site in northern Greenland (78 °N; **Fig. 5**) was ~0.8 mg m^{-2} a^{-1} (Lee et al., 2013), which is is 3-4 times larger than at the DV99.1 site over the same period, although the two sites are only distant by 750 km, lie at comparable altitudes (1985 and 1750 m a.s.l., respectively), and have the same mean $\dot{A}$ (0.14 m a^{-1}; Bales et

al., 2009). This suggests that the differences in F_{rBC} between these sites are related to spatial gradients in atmospheric BC burden in this sector of the Arctic.

As noted earlier, rBC concentrations in the DV99.1 core decreased gradually in the latter half of the 20th century, the change becoming most noticeable after the 1960s (**Fig. 4**). During this period, anthropogenic BC emissions decreased in Europe and North America, and air monitoring at Alert show that BC concentrations in surface air continued to decline following the early 1990s in response to reduced BC emissions (Gong et al., 2010). Reconstructed interannual changes in $\dot{A}$ on Devon ice cap by Colgan and Sharp (2008) do not reveal any sustained long-term trend for the period 1963-1990, and it is therefore unlikely that the decrease in rBC concentration registered in the DV99.1 core in this period can be ascribed to changing precipitation patterns on the ice cap. It is more probable that it reflects a declining burden of atmospheric BC in the Canadian High Arctic since the 1960s. In turn, this decline can be attributed to lower BC emissions, both anthropogenic and from BB, in dominant source regions, and, possibly, greater scavenging efficiency and wet deposition of BC during transport under a warming Arctic climate (Ruppel et al., 2014).

5 Summary and conclusions

We developed a 190-year time series of atmospheric rBC deposition from Devon ice cap spanning calendar years 1810-1990. The rBC ice core record (core DV99.1) is the first from the Canadian Arctic, and it supplements existing ice-core records of BC or EC deposition from Greenland and Svalbard. The time series differs from the Greenland records in that it shows no evidence of a substantial increase in rBC deposition during the early-mid 20th century, which, for Greenland, has been associated with coal combustion (McConnell et al., 2007). The deposition of other contaminants such as SO_4^{2-} and Pb did increase on the Devon ice cap in the latter half of the 20th century but without a concomitant rise in rBC.

We attribute the low baseline variability in rBC deposition in the DV99.1 core to both site-specific and regional-scale factors. The site from which the core was retrieved is subject to wind scouring and summer melt, and these combined effects probably lessen the amplitude and resolution of historical variations in rBC deposition recorded in firn at the site. Also, air back-trajectory analyses suggest that, compared to Greenland, rBC deposition on Devon ice cap is less sensitive to temporal changes in BC emissions from the North Atlantic sector (eastern North America and western Greenland). We postulate that BC aerosols reaching Devon ice cap originate more frequently from north-central/northwestern North America, and/or from Russia and central Asia. The relatively long transport trajectories over the Arctic Ocean allow for greater atmospheric mixing and deposition of aerosols to occur during transit, thus obscuring source-receptor relationships. If correct, this interpretation implies that historical trends in BC deposition over the Arctic, and the resulting albedo-climate forcing, are likely subject to large spatial variability, even over the relatively short distance that separates Devon ice cap from Greenland. This variability, which is probably linked to differences in BC aerosol transport patterns and atmospheric residence time (Bauer et al. 2013), must be accounted for when attempting to model the impact of past and future BC emission trends on the Arctic climate system.

Atmospheric
Chemistry
and Physics
Discussions

The discussion presented above also underscores the challenges of interpreting records of aerosol deposition developed from firn or ice cores drilled on small ice caps or glaciers, where local topographic and climatological effects can have a large impact on the preservation of atmospheric signals, when compared with the central regions of large ice sheets. A limitation of our study stems from the fact that the DV99.1 record of rBC deposition comes from a different site than records

5   of other aerosol species (SO_4^{2-}, Pb) previously obtained from Devon ice cap's summit. To verify our interpretation of the DV99.1 rBC record, a new core should be drilled from the ice cap's summit, or from another ice cap less affected by melt-percolation effects (e.g., on northern Ellesmere Island), and on which co-registered measurements of rBC and other aerosols could be made. This is particularly important when one considers the large amount of spatial variability inherent in ice core records, even in areas of optimal preservation (e.g., Gfeller et al., 2014). Our study also raises questions on the potential

10   effect of post-depositional coagulation of rBC particles on their detection by SP2 measurements in melted snow and ice samples. Experimental work is needed to clarify these effects.

Acknowledgements

References

AMAP. *Arctic Climate Issues 2015: Short-Lived Climate Pollutants: Summary for Policy-Makers*. Oslo: Arctic

20   Monitoring and Assessment Programme (AMAP), 16 pp., 2015

AMAP. *The Impact of Black Carbon on Arctic Climate.* Oslo: Arctic Monitoring and Assessment Programme
    (AMAP), 72 pp., 2012.

Ashbaugh, L.L., Malm, W.C., and Sadeh, W.Z. A residence time probability analysis of sulfur concentrations at Grand
    Canyon National Park: Atmos. Environ.,19, 1263–1270, doi:10.1016/0004-6981(85)90256-2, 1985.

25   Bales, R.C., Guo,Q., Shen, D., McConnell, J.R., Du,G., Burkhart, J.F., Spikes, V.B., Hanna, E. and Cappelen, J. Annual
    accumulation for Greenland updated using ice core data developed during 2000–2006 and analysis of daily coastal
    meteorological data. J. Geophys. Res., 114, D06116, doi:10.1029/2008JD011208, 2009.

Bauer, S.E., A. Bausch, L. Nazarenko, K. Tsigaridis, B. Xu, R. Edwards, M. Bisiaux, and J. McConnell. Historical and
    future black carbon deposition on the three ice caps: Ice-core measurements and model simulations from 1850 to

30   2100. J. Geophys. Res. Atmos., 118, 7948–7961, doi:10.1002/jgrd.50612, 2013.

Atmospheric
Chemistry
and Physics
Discussions

Benjamin, Y. and Yekutieli, S. The control of the false discovery rate in multiple testing under dependency. Ann.
    Stat., 29, 1165–1188, doi: 10.1214/aos/1013699998, 2001.

Bisiaux, M.M., Edwards, R., McConnell, J.R., Curran, M. A. J., Van Ommen, T.D., Smith, A.M., Neumann, T.A., Pasteris,

5   D.R., Penner, J.E., and Taylor, K. Changes in black carbon deposition to Antarctica from two high-resolution ice core
    records, 1850–2000 AD. Atmos. Chem. Phys., 12, 4107–4115, doi:10.5194/acp-12-4107-2012, 2012.

Bond, T.C., Doherty, S.J., Fahey, D.W., Forster, P.M., Berntsen, T., DeAngelo, B.J., Flanner, M.G., Ghan, S., Kärcher, B.,
    Koch, D., Kinne, S., Kondo, Y., Quinn, P.K., Sarofim, M.C., Schultz, M.G., Schulz, M., Venkataraman, C., Zhang, H.,
    Zhang, S., Bellouin, N., Guttikunda, S. K., Hopke, P.K., Jacobson, M.Z., Kaiser, J.W., Klimont, Z., Lohmann, U.,

10   Schwarz, J.P., Shindell, D., Storelvmo, T., Warren, S.G. and Zender, C.S. (2013) Bounding the role of black carbon in the
    climate system: A scientific assessment. J. Geophys. Res. Atmos., 118, 5380–5552, doi:10.1002/jgrd.50171, 2013.

Bond, T. C., Bhardwaj, E., Dong, R., Jogani, R., Jung, S. K., Roden, C., Streets, D. G., and Trautmann, N. M. Historical
    emissions of black and organic carbon aerosol from energy-related combustion, 1850–2000, Global Biogeochem. Cy., 21,
    Gb2018, doi:10.1029/2006gb002840, 2007.

15   Boon, S., Burgess, D.O., Koerner, R.M. and Sharp, M. J. Forty-seven years of research on the Devon Island ice cap, Arctic
    Canada. Arctic, 63, 13–29, 2010.

Browse, J., Carslaw, K.S., Arnold, S.R., Pringle, K. and Boucher, O. The scavenging processes controlling the seasonal
    cycle in Arctic sulphate and black carbon aerosol. Atmos. Chem. Phys., 12, 6775–6798, doi:10.5194/acp-12-6775-2012,
    2012.

20   Buchardt, S.L., Clausen, H.B., Vinther, B.M. and Dahl-Jensen, D. Investigating the past and recent ^{18}O-accumulation
    relationship seen in Greenland ice cores. Clim. Past, 8, 2053–2059, doi:10.5194/cp-8-2053-2012, 2012.

Cheng, M.D. Geolocating Russian sources for Arctic black carbon. Atmos. Environ., 92, 398–410,
    doi: 10.1016/j.atmosenv.2014.04.031, 2014.

Colgan, W. and Sharp, M. Combined oceanic and atmospheric influences on net accumulation on Devon Ice Cap, Nunavut,

25   Canada. J. Glaciol., 54, 28–40, doi:10.3189/002214308784409044, 2008.

Dansgaard, W. and Johnsen, S.J. A flow model and a time scale for the ice core from Camp Century, Greenland. J. Glaciol.,
    8, 215–223, doi:10.1017/S0022143000031208, 1969.

de la Peña, S., Howat, I.M., Nienow, P.W., van den Broeke, M.R., Mosley-Thompson, E., Price, S.F., Mair, D., Noël, B. and
    Sole, A.J. Changes in the firn structure of the western Greenland Ice Sheet caused by recent warming. Cryosphere, 9,

30   1203–1211, doi: 10.5194/tc-9-1203-2015, 2015.

Doherty, S.J., Grenfell, T.C., Forsström, S., Hegg, D.L., Brandt, R.E. and Warren, S.G. Observed vertical redistribution of
    black carbon and other insoluble light-absorbing particles in melting snow. J. Geophys. Res. Atmos., 118, 5553–5569,
    doi:10.1002/jgrd.50235, 2013.

Doherty, S. J., Warren, S. G., Grenfell, T. C., Clarke, A. D. and Brandt, R. E. Light-absorbing impurities in Arctic snow.

Atmos. Chem. Phys., 10, 11,647–11,680, doi:10.5194/acp-10-11647-2010, 2010.

Draxler, R.R. and Hess, G.D. *Description of the HYSPLIT 4 modeling system.* NOAA Technical Memorandum ARL-224. Air Resources Laboratory, Silver Spring, Maryland, USA, 27 p., 2014.

Fisher, D. A. and Koerner, R. M. Signal and noise in four ice-core records from the Agassiz Ice Cap, Ellesmere Island,
5   Canada: details of the last millennium for stable isotopes, melt and solid conductivity. Holocene, 4, 113–120 doi, 1994.

Fisher, D. A. and Koerner, R. M. The effects of wind on $\delta^{18}O$ and accumulation give an inferred record of seasonal amplitude from the Agassiz Ice Cap, Ellesmere Island, Canada. Ann. Glaciol., 10, 34–37, doi:10.1017/S0260305500004122, 1988.

Fisher, D.A., Reeh, N. and Clausen, H.B. Stratigraphic noise in time series derived from ice cores. Ann. Glaciol., **7**,
10   76–83, doi:10.1017/S0260305500005942, 1985.

Fisher, D.A., Zheng, J., Burgess, D., Zdanowicz, C., Kinnard, C., Sharp, M. and Bourgeois, J. Recent melt rates of Canadian Arctic ice caps are the highest in four millennia. Global Planet. Change, 84–85, 3–7, doi:10.1016/j.gloplacha.2011.06.005, 2012.

Fisher, D. A., Koerner, R. M., Paterson, W. S. B., Dansgaard, W., Gundestrup, N. and Reeh, N. Effect of wind scouring on
15   climatic records from ice-core oxygen-isotope profiles. Nature, 301, 205–209, doi:10.1038/301205a0, 1983.

Garrett, T.J., Brattström, S., Sharma, S., Worthy, D.E.J., and Novelli, P. The role of scavenging in the seasonal transport of black carbon and sulfate to the Arctic. Geophys. Res. Lett., 38, L16805, doi:10.1029/2011GL048221, 2011.

Giradin, M.P. Interannual to decadal changes in area burned in Canada from 1781 to 1982 and the relationship to Northern Hemisphere land temperatures. Global Ecol. Biogeogr., 16, 557–566, doi:10.1111/j.1466-8238.2007.00321.x, 2007.

20   Girardin, M. and Sauchyn, D. Three centuries of annual area burned variability in northwestern North America inferred from tree rings. Holocene, 18, 205–214, doi: 10.1177/0959683607086759, 2008.

Girardin, M.P., Bergeron, Y., Tardif, J.C., Gauthier, S., Flannigan, M.D. and Mudelsee, M. 229-year dendroclimatic-inferred record of forest fire activity for the Boreal Shield of Canada. Int. J. Wildland Fire, 15, 375–388, doi:10.1071/WF05065, 2006.

25   Gfeller, G., Fischer, H., Bigler, M., Schüpbach, S., Leuenberger, D. and Mini, O. Representativeness and seasonality of major ion records derived from NEEM firn cores. Cryosphere, 8, 1855–1870, doi:10.5194/tc-8-1855-2014, 2014.

Gong, S. L., Zhao,T. L., Sharma, S., Toom-Sauntry, D., Lavoué, D., Zhang, X. B., Leaitch, W. R. and Barrie, L. A. Identification of trends and interannual variability of sulfate and black carbon in the Canadian High Arctic: 1981–2007. J. Geophys. Res., 115, doi:10.1029/2009JD012943, 2010.

30   Goto-Azuma, K. and Koerner, R.M. Ice core studies of anthropogenic sulfate and nitrate trends in the Arctic. J. Geophys. Res., 206, D5, 4959–69, doi:10.1029/2000JD900635, 2001.

Hirdman, D., Burkhart, J.F., Sodemann, H., Eckhardt, S., Jefferson, A., Quinn, P.K., Sharma, S., Ström, J. and Stohl, A. Long-term trends of black carbon and sulphate aerosol in the Arctic: changes in atmospheric transport and source region emissions. Atmos. Chem. Phys., 10, 9351–9368, doi:10.5194/acp-10-9351-2010, 2010.

Atmospheric
Chemistry
and Physics
Discussions

Huang, L., Gong, S. L., Sharma, S., Lavoué, D. and Jia1, C. Q. A trajectory analysis of atmospheric transport of black carbon aerosols to Canadian high Arctic in winter and spring (1990–2005). Atmos. Chem. Phys., 10, 5065–5073, doi:10.5194/acp-10-5065-2010, 2010.

5 Kassomenos, P., Vardoulakis, S., Borge, R., Lumbreras, J., Papaloukas, C. and Karakitsios, S. Comparison of statistical clustering techniques for the classification of modelled atmospheric trajectories. Theor. Appl. Climatol., 102, 1–12, doi:10.1007/s00704-009-0233-7, 2010.

Kinnard, C., Zdanowicz, C.M., Fisher, D.A., Wake, C.P. Calibration of an ice-core glaciochemical (sea-salt) record with sea-ice variability in the Canadian Arctic. Ann. Glaciol., 44, 383–390, doi:10.3189/172756406781811349, 2010.

10 Kistler, R., Kalnay, E., Collins, W., Saha, S., White, G., Woollen, J., Chelliah, M., Ebisuzaki, W., Kanamitsu, M., Kousky, V., Van Den Dool, H., Jenne, R. and Fiorino, M. The NCEP-NCAR 50-year reanalysis: Monthly means CD-ROM and documentation. B. Am. Meteorol. Soc., 82, 2, 247-267, doi:10.1175/1520-0477(2001)082<0247:TNNYRM>2.3.CO;2, 2001.

Koch, K., Bauer, S.E., Del Genio, A., Faluvegi, G., McConnell, J.R., Menon, S., Miller, R.L., Rind, D., Ruedy, R., Schmidt,
15 G.A. and Shindell, D. Coupled aerosol-chemistry–climate twentieth-century transient model investigation: Trends in short-lived species and climate responses. J. Climate, 24, 2693–2714, doi: 10.1175/2011JCLI3582.1, 2011.

Jiao C. and Flanner, M.G. Changing black carbon transport to the Arctic from present day to the end of 21st century. J. Geophys. Res. Atmos., 121, 4734–4750, doi:10.1002/2015JD023964, 2016.

Jiao, C., Flanner, M.G., Balkanski, Y., Bauer, S.E., Bellouin, N., Berntsen, T.K., Bian, H., Carslaw, K.S., Chin, M., De
20 Luca, N., Diehl, T., Ghan, S.J., Iversen, T., Kirkevåg, A., Koch, D., Liu, X., Mann, G.W., Penner, J.E., Pitari, G., Schulz, M., Seland, Ø., Skeie, R.B., Steenrod, S.D., Stier, P., Takemura, T., Tsigaridis, K., van Noije, T., Yun, Y., and Zhang, K. An AeroCom assessment of black carbon in Arctic snow and sea ice. Atmos. Chem. Phys., 14, 2399–2417, doi:10.5194/acp-14-2399-2014, 2014.

Lamarque, J.F., Bond, T.C., Eyring, V., Granier, C., Heil, A., Klimont, Z., Lee, D., Liousse, C., Mieville, A., Owen, B.,
25 Schultz, M.G., Shindell, D., Smith, S.J., Stehfest, E.,Van Aardenne, J., Cooper, O.R., Kainuma, M., Mahowald, N., McConnell, J.R., Naik, V., Riahi, R. and van Vuuren, D.P. Historical (1850–2000) gridded anthropogenic and biomass burning emissions of reactive gases and aerosols: methodology and application. Atmos. Chem. Phys., 10, 7017–7039, doi:10.5194/acp-10-7017-2010, 2010.

Lee, Y.H., Lamarque, J.F., Flanner, M.G., Jiao, C., Shindell, D.T., Berntsen, T., Bisiaux, M.M., Cao, J., Collins, W.J.,
30 Curran, M., Edwards, R., Faluvegi, G., Ghan, S., Horowitz, L.W., McConnell, J.R., Ming, J., Myhre, G., Nagashima, T., Naik, V., Rumbold, S.T., Skeie, R.B., Sudo, K., Takemura, T., Thevenon, F., Xu, B. and Yoon, J.-H. Evaluation of preindustrial to present-day black carbon and its albedo forcing from Atmospheric Chemistry and Climate Model Intercomparison Project (ACCMIP). Atmos. Chem. Phys., 13, 2607–2634, doi:10.5194/acp-13-2607-2013, 2013.

Legrand, M., McConnell, J. Fischer, H., Wolff, E. W., Preunkert, S., Arienzo, M., Nathan Chellman, N., Leuenberger, D., Maselli, O., Place, P., Sigl, M., Schüpbach, S. and Flannigan, M. Boreal fire records in Northern Hemisphere ice cores: a review. Clim. Past., 12, 2033–2059, doi:10.5194/cp-12-2033-2016, 2016.

5 Liu, D., Allan, J., Whitehead, J., Young, D., Flynn, M., Coel, H., McFiggans, G., Fleming, Z.L. and Bandy, B. Ambient black carbon particle hygroscopic properties controlled by mixing state and composition. Atmos. Chem. Phys., 13, 2015–2029, doi:10.5194/acp-13-2015-2013, 2013.

Liu, J., Fan, S., Horowitz, L.W. and Levy, H. Evaluation of factors controlling long-range transport of black carbon to the Arctic. J. Geophys. Res., 116, D04307, doi:10.1029/2010JD015145, 2011.

10 Machguth, H., MacFerrin, M., van As, D., Box, J.E., Charalampidis, C., Colgan, W., Fausto, R.S., Meijer, H.A.J., Mosley-Thompson, E. and van deWal, R.S.W. Greenland meltwater storage in firn limited by near-surface ice formation. Nat. Clim. Change, 6, doi:10.1038/NCLIMATE2899, 2016.

Massling, A., Nielsen, I. E., Kristensen, D., Christensen, J. H., Sørensen, L. L., Jensen, B., Nguyen, Q. T., Nøjgaard, J. K., Glasius, M. and Skov, H. Atmospheric black carbon and sulfate concentrations in Northeast Greenland. Atmos.

15 Chem. Phys., 15, 9681–9692, doi:10.5194/acp-15-9681-2015, 2015.

McConnell, J. R. New directions: Historical black carbon and other ice core aerosol records in the Arctic for GCM evaluation. Atmos. Environ., 44, 2665–2666, 10.1016/j.atmosenv.2010.04.004, 2010.

McConnell, J. R. and Edwards, R. Coal burning leaves toxic heavy metal legacy in the Arctic. P. Natl. Acad. Sci. USA, 105, 12,140–12,144, doi:10.1073/pnas.0803564105, 2008.

20 McConnell, J. R., Edwards, R., Kok, G. L., Flanner, M. G., Zender, C. S., Saltzman, E. S., Banta, J. R., Pasteris, D. R., Carter, M. M., and Kahl, J.D. 20th-century industrial black carbon emissions altered Arctic climate forcing. Science, 317, 1381–1384, doi:10.1126/science.1144856, 2007.

Miller, J.E., Kahl, J.D.W., Heller, F. and Harris, J.M. A three-dimensional residence-time analysis of potential summertime atmospheric transport to Summit, Greenland. Ann. Glaciol., 35, 403–408, doi:10.3189/172756402781816663, 2002.

25 Mouillot, F. and Field, C. B. Fire history and the global carbon budget: a 1×1° fire history reconstruction for the 20th century. Glob. Change Biol., 11,398–11,420, doi:10.1111/j.1365-2486.2005.00920.x, 2005.

Novakov, T., Ramanathan, V., Hansen, J.E., Kirchstetter, T.W., Sato, M., Sinton, J.E. and Sathaye, J.A. Large historical changes of fossil-fuel black carbon aerosols. Geophys. Res. Lett., 30, 1324, doi:10.1029/2002GL016345, 2003.

Paris, J.-D., Stohl, A., Nédélec, P., Arshinov, M. Yu., Panchenko, M.V., Shmargunov, V.P., Law, K.S., Belan, B.D. and

30 Ciais, P. Wildfire smoke in the Siberian Arctic in summer: source characterization and plume evolution from airborne measurements. Atmos. Chem. Phys., 9, 9315–9327, doi:10.5194/acp-9-9315-2009, 2009.

Petzold, A., Ogren, J.A., Fiebig, M., Laj, P., Li, S.-M., Baltensperger, U., Holzer-Popp, T., Kinne, S., Pappalardo, G., Sugimoto, N., Wehrli, C., Wiedensohler, A. and Zhang, X.-Y. Recommendations for reporting "black carbon" measurements. Atmos. Chem. Phys., 13, 8365–8379, doi:10.5194/acp-13-8365-2013, 2013.

Pilson, M. E. O. *An Introduction to the Chemistry of the Sea*, 2nd edition. Cambridge: Cambridge University Press, 533 pp., 2012.

Quennehen, B., Schwarzenboeck, A., Matsuki, A., Burkhart, J.F., Stohl, A., Ancellet, G. and Law, K.S. Anthropogenic and
5   forest fire pollution aerosol transported to the Arctic: observations from the POLARCAT-France spring campaign. Atmos. Chem. Phys., 12, 6437–6454, doi:10.5194/acp-12-6437-2012, 2012.

Quinn, P.K., Bates, T.S., Baum, E., Doubleday, N., Fiore, A.M., Flanner, M., Fridlind, A., Garrett, T.J., Koch, D., Menon, S., Shindell, D., Stohl, A. and Warren, S.G. Short-lived pollutants in the Arctic: their climate impact and possible mitigation strategies. Atmos. Chem. Phys., 8, 1723–1735, doi:10.5194/acp-8-1723-2008, 2008.

10   Raut, J.-C., Marelle, L., Fast, J.D., Thomas, J.L., Weinzierl, B., Law, K.S., Berg, L.K., Roiger, A., Easter, R.C., Heimer, K., Onishi, T., Delanoë1, J. and Schlager, H. Cross-polar transport and scavenging of Siberian aerosols containing black carbon during the 2012 ACCESS summer campaign, Atmos. Chem. Phys., 17, doi:10.5194/acp-17-10969-2017, 2017.

Ruppel, M.M., Isaksson, I., Ström, J., Beaudon, E., Svensson, J., Pedersen, C.A. and Korhola, A. Increase in elemental carbon values between 1970 and 2004 observed in a 300-year ice core from Holtedahlfonna (Svalbard). Atmos. Chem.
15   Phys., 14, 11,447–11,460, doi:10.5194/acp-14-11447-2014, 2014.

Ruth, U., Wagenbach, D., Steffensen, J. P. and Bigler, M. Continuous record of microparticle concentration and size distribution in the central Greenland NGRIP ice core during the last glacial period. J. Geophys. Res., 108, 1–12, doi:10.1029/2002JD002376, 2003.

Schwarz, J.P., Gao, R.S., Perring, A.E., Spackman, J.R. and Fahey, D.W. Black carbon aerosol size in snow. Sci. Rep., 3,
20   1356, doi:10.1038/srep01356, 2013.

Schwarz, J. P., Doherty, S. J., Li, F., Ruggiero, S. T., Tanner, C.E., Perring, A. E., Gao, R. S., and Fahey, D. W. Assessing single particle soot photometer and integrating sphere / integrating sandwich spectrophotometer measurement techniques for quantifying black carbon concentration in snow. Atmos. Meas. Tech., 5, 2581–2592, doi:10.5194/amt-5-2581-2012, 2012.

25   Schwarz, J.P., Spackman, J.R., Gao, R.S., Perring, A.E., Cross, E., Onasch, T.B., Ahern, A., Wrobel, W., Davidovits, P., Olfert, J., Dubey, M.K., Mazzoleni, C., and Fahey, D.W. The detection efficiency of the single particle soot photometer. Aerosol Sci. Tech., 44, 612–628, doi:10.1080/02786826.2010.481298, 2010.

Sharma, S., Andrews, E., Barrie, L. A., Ogren, J. A. and Lavoué, D. Variations and sources of the equivalent black carbon in the High Arctic revealed by long-term observations at Alert and Barrow: 1989–2003. J. Geophys. Res., 111, D14208,
30   doi:10.1029/2005JD006581, 2006.

Shen, Z., Ming, Y., Horowitz, L.W., Ramaswamy, V. and Lin, M. On the seasonality of Arctic black carbon. J. Climate, 30, 4429-4441, doi:1 0.1175/JCLI-D-16-0580.1, 2017.

Shotyk, W., Zheng, J., Krachler, M., Zdanowicz, C., Koerner, R. and Fisher, D. Predominance of industrial Pb in recent snow (1994–2004) and ice (1842–1996) from Devon Island, Arctic Canada. Geophys. Res. Lett., 32,

Atmospheric
Chemistry
and Physics
Discussions

doi:10.1029/2005GL023860, 2005.

Schultz, M. G., Heil, A., Hoelzemann, J. J., Spessa, A., Thonicke, K., Goldammer, J., Held, A. C., Pereira, J. M., and van het Bolscher, M. Global Wildland Fire Emissions from 1960 to 2000. Global Biogeochem. Cy., 22, GB2002, doi:10.1029/2007GB003031, 2008.

5 Shindell, D.T., Chin, N., Dentener, F., Doherty, R.M., Faluvegi, G., Fiore, A.M., Hess, P., Koch, D.M., MacKenzie, I.A., Sanderson, M.G., Schultz, M.G., Schulz, M., Stevenson, D.S., Teich, H., Textor, C., Wild, O., Bergman, D.J., Bey, I., Bian, H., Cuvelier, C., Duncan, B.N., Folberth, G., Horowitz, L.W., Jonson, J., Kaminski, J.W., Marmer, E., Park, R., Pringle, K.J., Szopa, S., Takemura, T., Zeng, G., Keating, T.J. and Zuber, A. A multi-model assessment of pollution transport to the Arctic. Atmos. Chem. Phys., 8, 5353–5372, doi: 10.5194/acp-8-5353-2008, 2008.

10 Simoneit, B.R.T. Biomass burning: A review of organic tracers for smoke from incomplete combustion. Appl. Geochem., 17: 129–162, doi:10.1016/S0883-2927(01)00061-0, 2002.

Skeie, R.B., Berntsen, T., Myhre, G., Pedersen, C.A., Ström, J., Gerland, S. and Ogren, J.A. Black carbon in the atmosphere and snow, from pre-industrial times until present. Atmos. Chem. Phys., 11, 6809–6836, doi:10.5194/acp-11-6809-2011, 2011.

15 Sigl, M., Winstrup, M., McConnell, J.R., Welten, K.C., Plunkett, G., Ludlow, F., Büntgen, U., Caffee, M., Chellman, N., Dahl-Jensen, D., Kipfstuhl, S., Kostick, C., Maselli, O.J., Mekhaldi, F., Mulvaney, R., Muscheler, R., Pasteris, D.R., Pilcher, J.R., Salzer, M., Schüpbach, S., Steffensen, J.P., Vinther, B.M. and Woodruff, T.E. Timing and climate forcing of volcanic eruptions for the past 2,500 years. Nature, 523, 543–549, doi:10.1038/nature14565, 2015.

Stein, A. F., Draxler, R. R., Rolph, G. D., Stunder, B. J. B., Cohen, M. D. and Ngan, F. NOAA's HYSPLIT atmospheric
20 transport and dispersion modeling system. B. Am. Meteorol. Soc., 96, 2050-2077, doi:10.1175/BAMS-D-14-00110.1, 2015.

Stohl, A., Andrews, E., Burkhart, J.F., Forster, C., Herber, A., Hoch, S.W., Kowal, D., Lunder, C., Mefford, T., Ogren, J.A., Sharma, S., Spichtinger, N., Stebel, K., Stone, R., Ström, J.,Tørseth, K., Wehrli, C. and Yttri, K.E. Pan-Arctic enhancements of light absorbing aerosol concentrations due to North American boreal forest fires during summer 2004.
25 J. Geophys. Res., 111, doi:10.1029/2006JD007216, 2006.

Su, L., Yuan, Z., Fung, J.C.H. and Lau, A.K.H. A comparison of HYSPLIT backward trajectories generated from two GDAS datasets. Sci. Total Environ., 506–507, 527–537, doi:10.1016/j.scitotenv.2014.11.072, 2015.

Vasileva, A.V., Moiseenko, K.B., Mayer, J.-C., Jürgens, N., Panov, A., Heimann, M. and Andreae, M. O. Assessment of the regional atmospheric impact of wildfire emissions based on CO observations at the ZOTTO tall tower station in central
30 Siberia. J. Geophys. Res., 116, D07301, doi:10.1029/2010JD014571, 2011.

Warneke, C., Bahreini, R., Brioude, J., Brock, C.A., de Gouw, A. Fahey, D.W., Froyd, K.D., Holloway, J.S., Middlebrook, A., Miller, L., Montzka, S., Murphy, D.M., Peischl, J., Ryerson, T.B., Schwarz, J.P., Spackman, J.R. and P. Veres. Biomass burning in Siberia and Kazakhstan as an important source for haze over the Alaskan Arctic in April 2008. J. Geophys. Res., 36, doi:10.1029/2008GL036194, 2009.

Wendl, I.A., Menking, J.A., Färber, R., Gysel, M., Kaspari, S.D., Laborde, M.J.G. and Schwikowski, M. Optimized method for black carbon analysis in ice and snow using the Single Particle Soot Photometer. Atmos. Measur. Tech., 7, 2667–2681, doi:10.5194/amt-7-2667-2014, 2014.

5 Wentworth, G.R., Murphy, J.G., Croft, B., Martin, R.V., Pierce, J.R., Côté, J.-S., Courchesne, I., Tremblay, J.-É., Gagnon, J., Thomas, J.L., Sharma, S., Toon-Saundry, D., Chivulescu, A., Levasseur, M. and Abbatt, J.P.D. Ammonia in the summertime Arctic marine boundary layer: sources, sinks, and implications. Atmos. Chem. Phys., 16, 1937–1953, doi:10.5194/acp-16-1937-2016, 2016.

Wilk, D.S. "The Stippling Shows Statistically Significant Grid Points": How research results are routinely overstated and
10 overinterpreted, and what to do about it. B. Am. Meteorol. Soc., 97, 12, 2263-2273, doi:10.1175/BAMS-D-15-00267.1, 2016.

Zennaro, P., Kehrwald, N., McConnell, J.R., Schüpbach, S., Maselli, O.J., Marlon, J., Vallelonga, P., Leuenberger, D., Zangrando, R., Spolaor, A., Borrotti, M., Barbaro, E., Gambaro, A. and Barbante, C. Fire in ice: two millennia of boreal forest fire history from the Greenland NEEM ice core. Clim. Past, 10, 1905–1924, doi:10.5194/cp-10-1905-2014, 2014.

15 Zheng, J., Kudo. A., Fisher. D., Blake. E. and Gerasimoff. M. Solid electrical conductivity (ECM) from four Agassiz ice cores, Ellesmere Island NWT, Canada: high-resolution signal and noise over the last millennium and low resolution over the Holocene. Holocene, 8, 413–421, doi: 10.1191/095968398676187747, 1998.
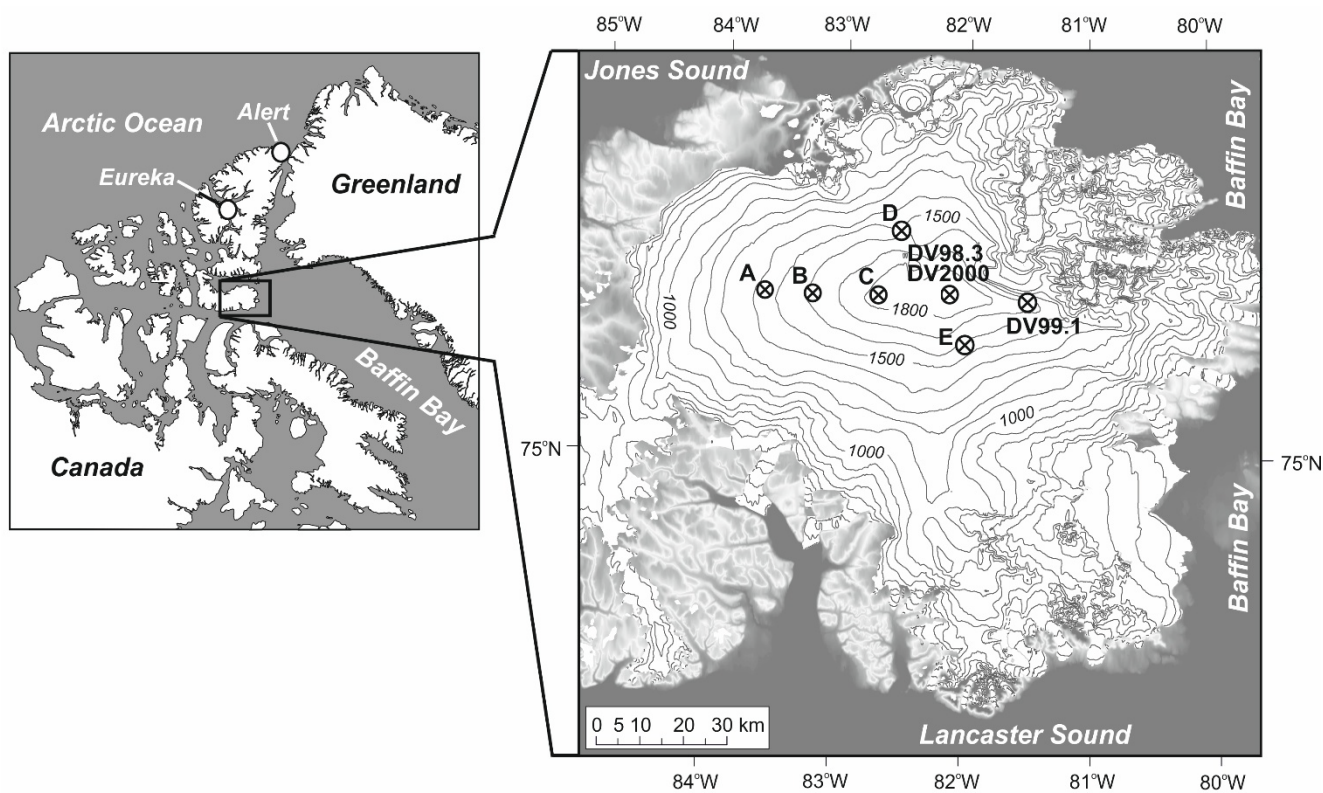
Figure 1: Location map of the Canadian Arctic Archipelago (left), with enlargement of Devon ice (right). The location of the various ice core sites mentioned in the text are shown. Sites A to E refer to the shallow core array of Colgan and Sharp (2008).
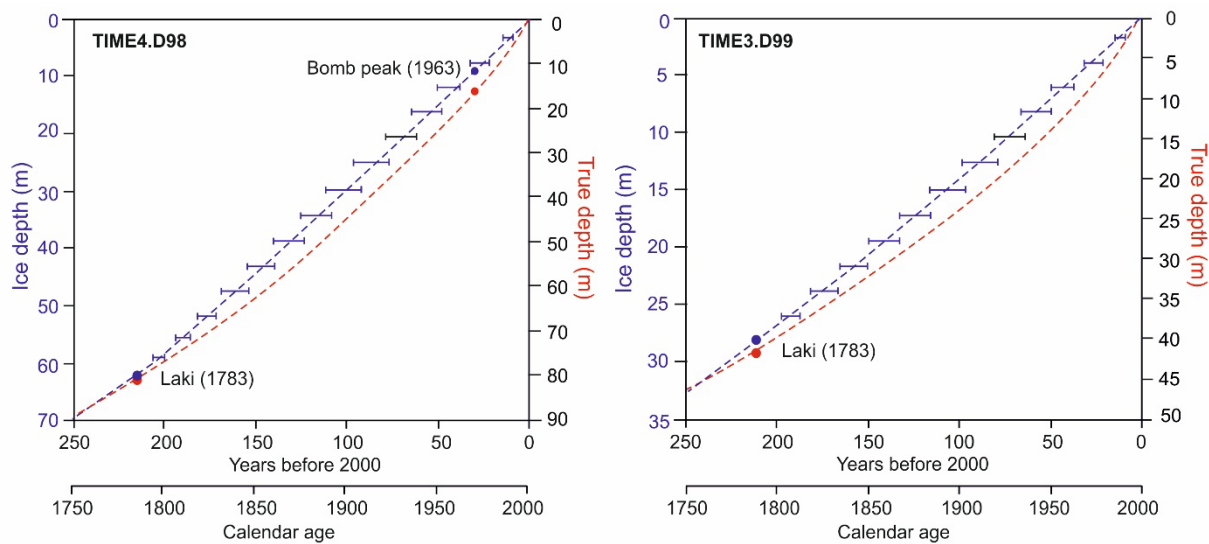5 **Elevation contours on Devon ice cap are spaced at 100 m above sea level.**

Figure 2: Age models for parts of the DV98.3 and DV99.1 cores from Devon ice cap. The error bars on the age curve relative to ice depths (blue) bracket the 95 % confidence interval as established from Monte Carlo simulations (see text).

5
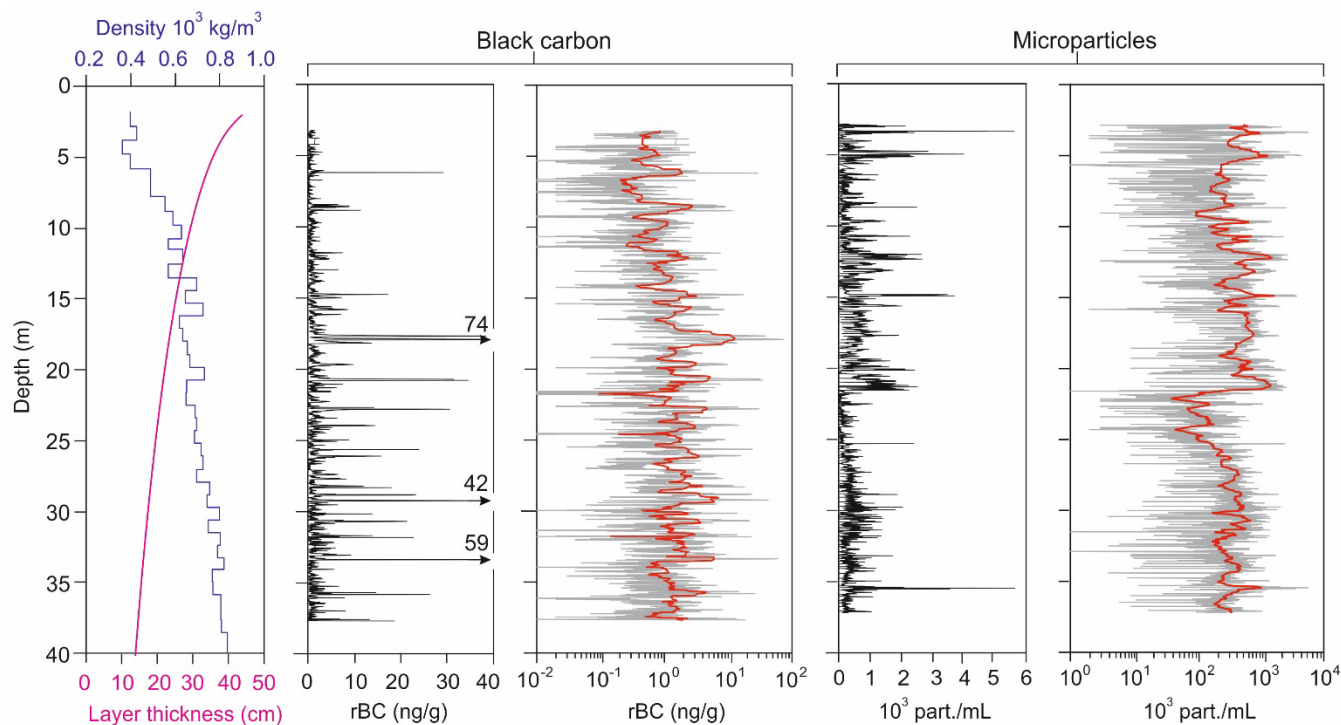
Figure 3: Depth profiles of physical properties and impurity concentrations in the top 38 m of the DV99.1 core. Left: Firn density and estimated mean annual layer thickness. Center: rBC concentrations shown on linear and log scales. The red line is a 500-point (~1-m) moving average. Right: Insoluble microparticle concentrations (0.9-15 μm diameter) on linear and log scales as for rBC.

5
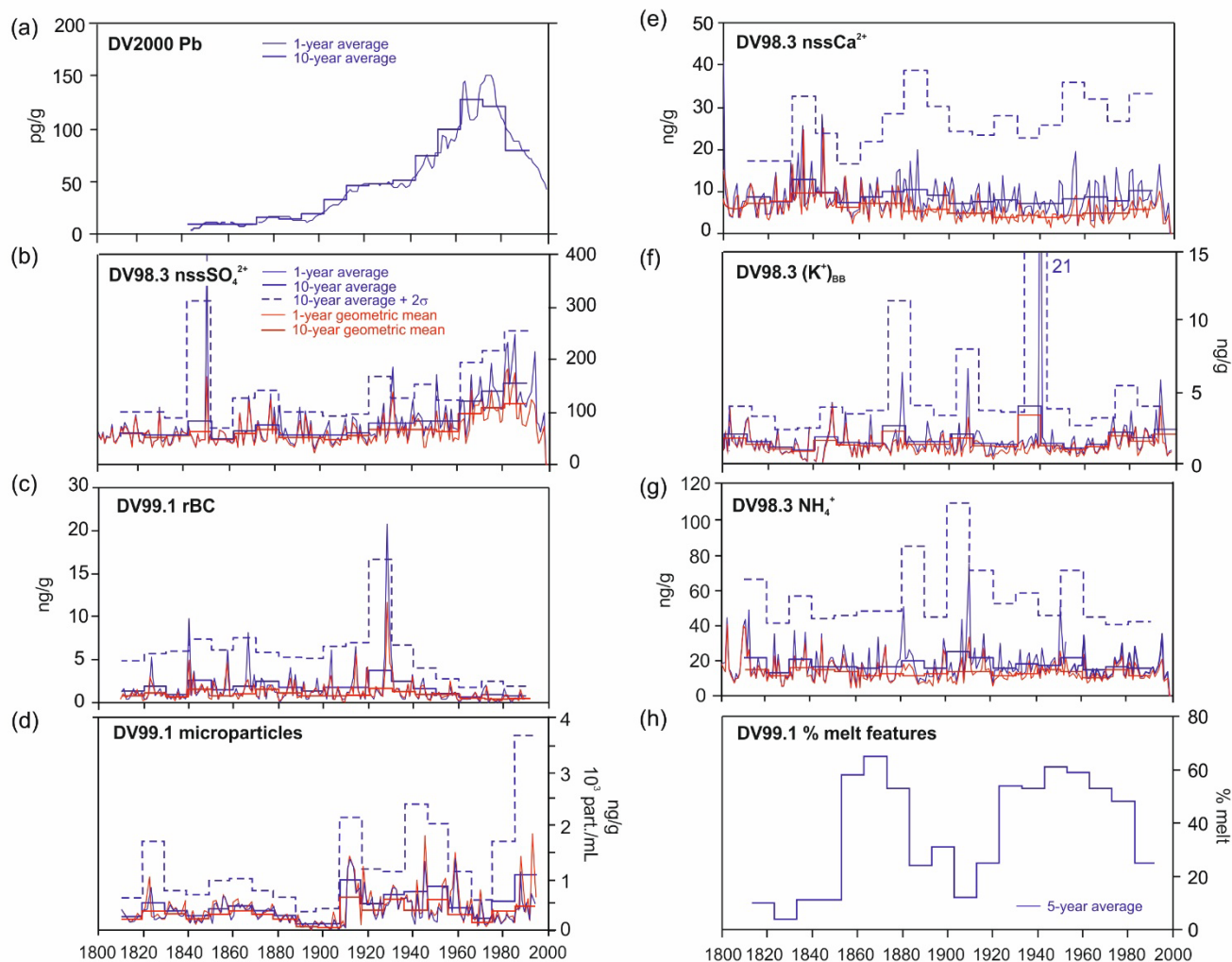
Figure 4: Historical changes in chemical and physical properties in firn and ice from Devon ice cap between the early 19th century and late 20th century: (a) Pb concentrations in the DV2000 core; (b) nssSO$_4^{2-}$ in the DV98.3 core; (c) rBC and (d) microparticle concentrations in the DV99.1 core; (e)-(g) nssCa^{2+}, (K$^+$)$_{BB}$ and NH$_4^+$ in the DV98.3 core; (h) volumetric percentage of surface melt in the DV99.1 core. Data from the DV2000 core are from from Shotyk et al. **(2005), while data from the DV98.3 core from Kinnard** et al. **(2006). Melt percentages in the DV99.1 core are from Fisher** et al. **(2012). For rBC, microparticles and ions, the arithmetic (blue) and geometric (red) mean are shown over one- and ten-year intervals. The upper limit of the 95% confidence interval (2σ) on decadal averages takes into account uncertainties in the ice-core age models, as well as those arising from the spatial variability in the distribution of atmospheric impurities across Devon ice cap (see text).**
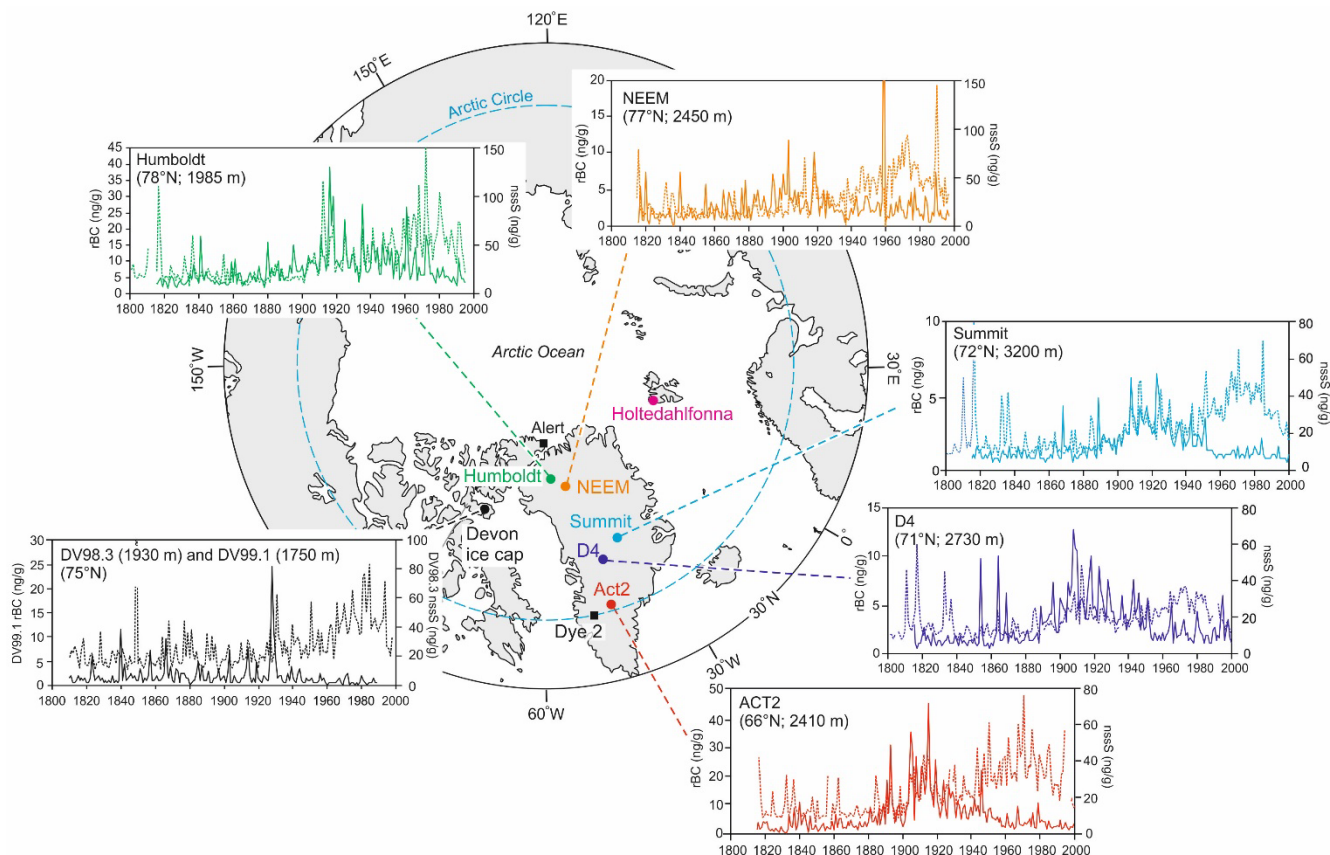
Figure 5: The record of atmospheric rBC and non-sea salt sulfur (nssS) deposition on Devon ice cap over the period 1810-2000 compared with similar records developed at various sites over Greenland by identical or nearly-identical methods. Full lines are rBC; stippled lines are nssS. Data from Summit, D4, ACT2 and Humboldt: McConnell et al., (2007) and Koch et al. (2011); data from NEEM: Zennaro et al. (2014) and Sigl et al. (2015). Also shown is the location of the ice-core record of elemental carbon (EC) deposition developed from Holtedahlfonna, Svalbard, by Ruppel et al. (2014), as well as other sites (Alert, Dye 2) mentioned in the text.
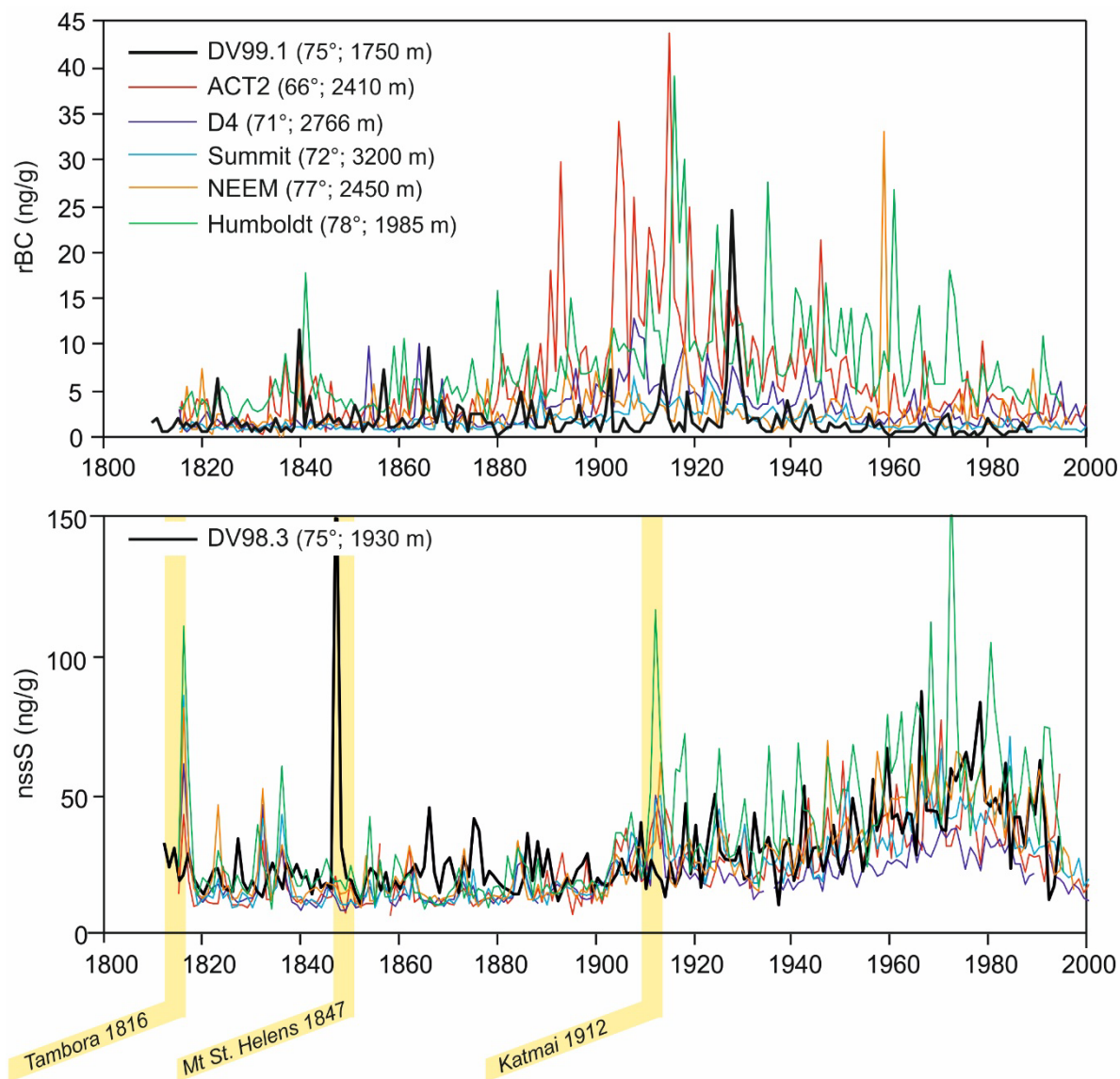
Figure 6: (a) The DV99.1 record of rBC deposition compared with other records developed from sites in Greenland identified in Fig. 5. All records are presented in one-year averages. (b) As in (a) but for records of non-sea salt sulfur (nssS). Three major historical volcanic eruption signals used for correlation are highlighted.
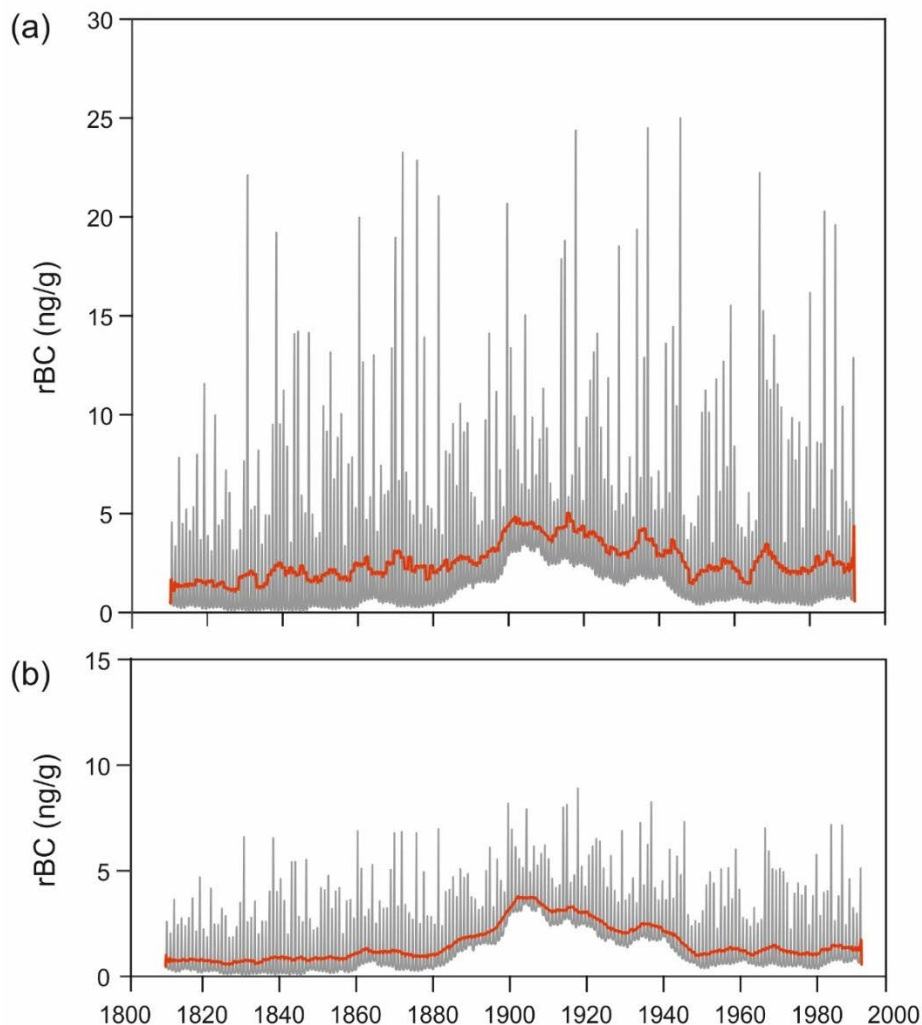
Figure 7: Simulation of the effects of snow wind scouring on the preservation of an anthropogenic signal of rBC deposition in a synthetic ice-core times series of rBC spanning the period 1810-1990. (a) The synthetic series, with a pseudo-seasonal cycle superimposed on the interdecadal baseline trend observed in the Greenland D4 record (McConnell et al., 2007). (b) The synthetic series after randomly truncating the amplitude of all winter deposition peaks (November-March) by 30-60 %. The bold red line in both panels is a 5-year running geometric mean.
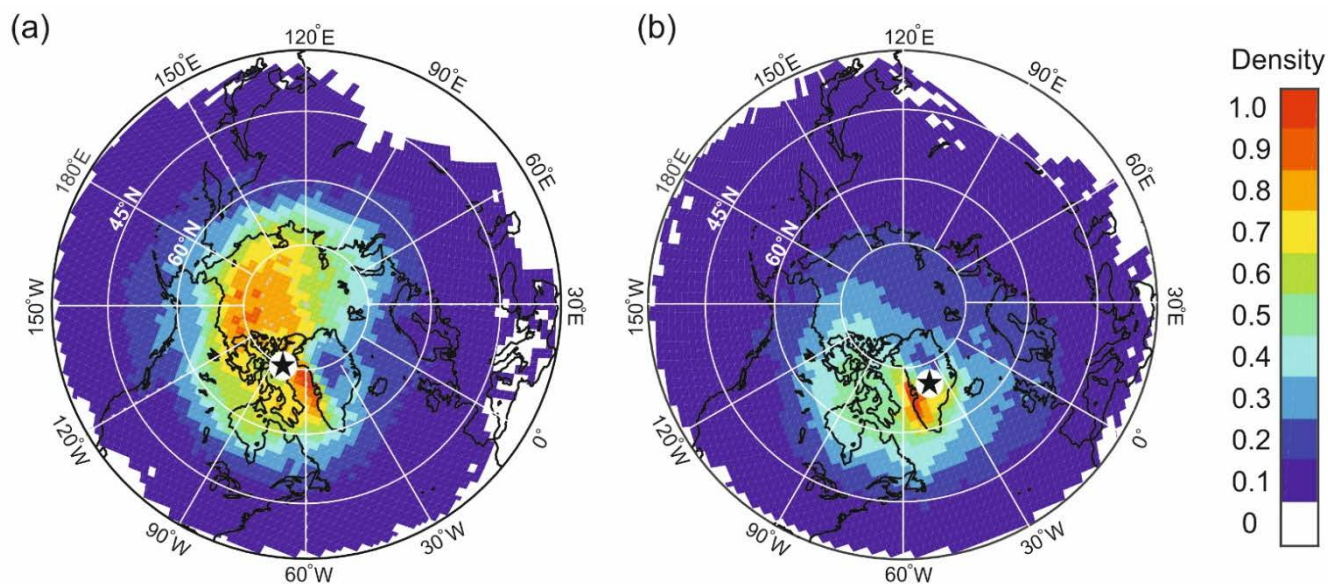
Figure 8: Maps of residence time probability for air arriving at (a) Devon ice cap and (b) Summit, Greenland over the period 1948-1999, computed using HYSPLIT4. Air residence probability densities were normalized to a scale of 0-1, and were spatially detrended by multiplying the original residence time grids (in hours) by the distance between each grid point and the coring site. This effectively removes the concentric increase in probability density near the back-trajectory start point (Ashbaugh et al., 1985). The spatial resolution of the grid is 200 × 200 km. The lower panels show the residence time density over time and as a function of altitude (m a.s.l.) for the two sites.

Atmospheric
Chemistry
and Physics
Discussions
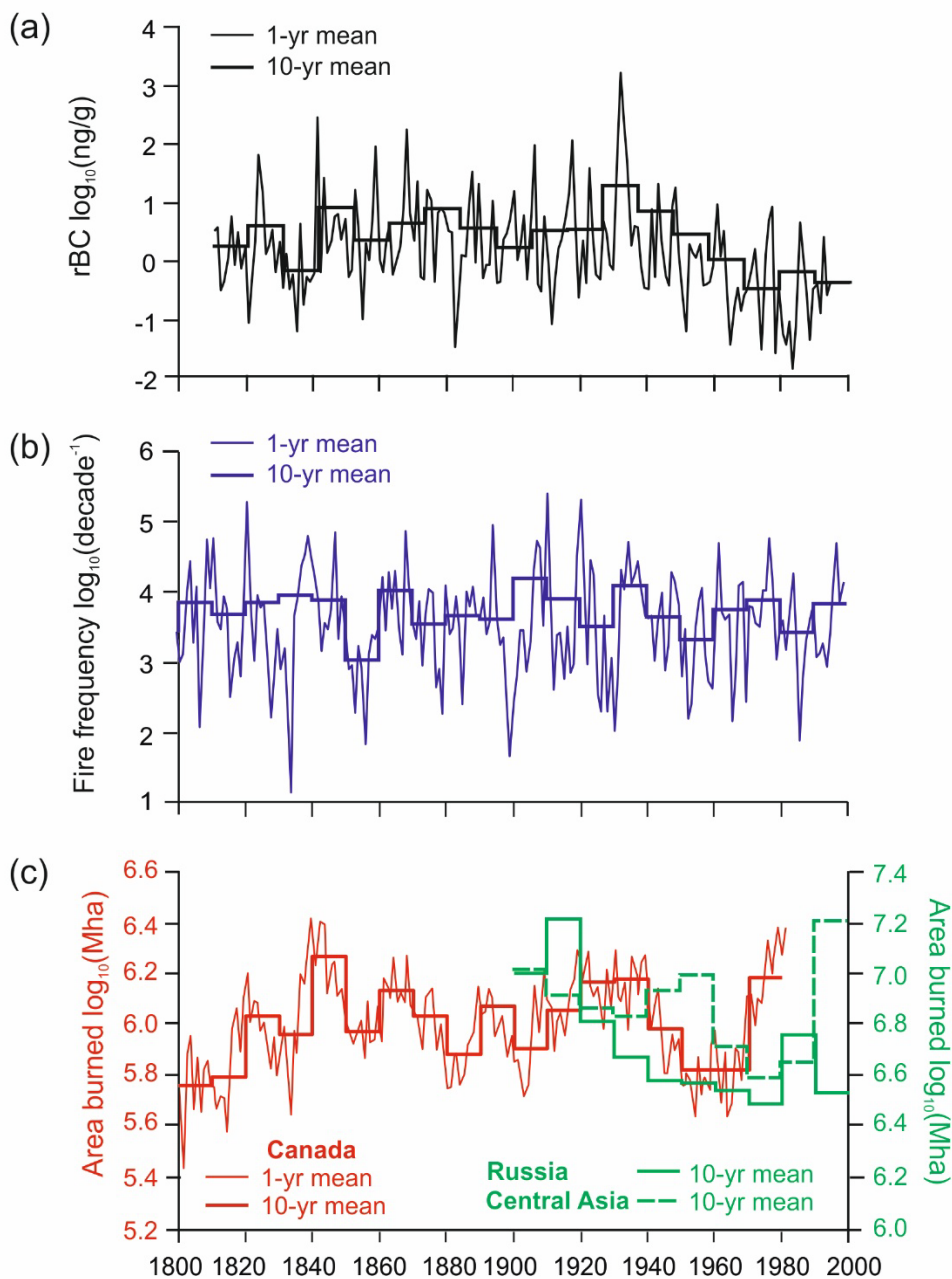
Figure 9: (a) Historical variations in rBC concentration in the DV99.1 core, 1810-1990, compared with reconstructed historical trends in **(b)** fire frequency in the eastern boreal forest region of Canada (Girardin et al., **2006**), and **(c)** burned area across northern Canada (Girardin, **2007**) and in the boreal and grassland regions of Russia and Central Asia (Mouillot and Field, **2005**). All data were log-transformed to facilitate comparisons.
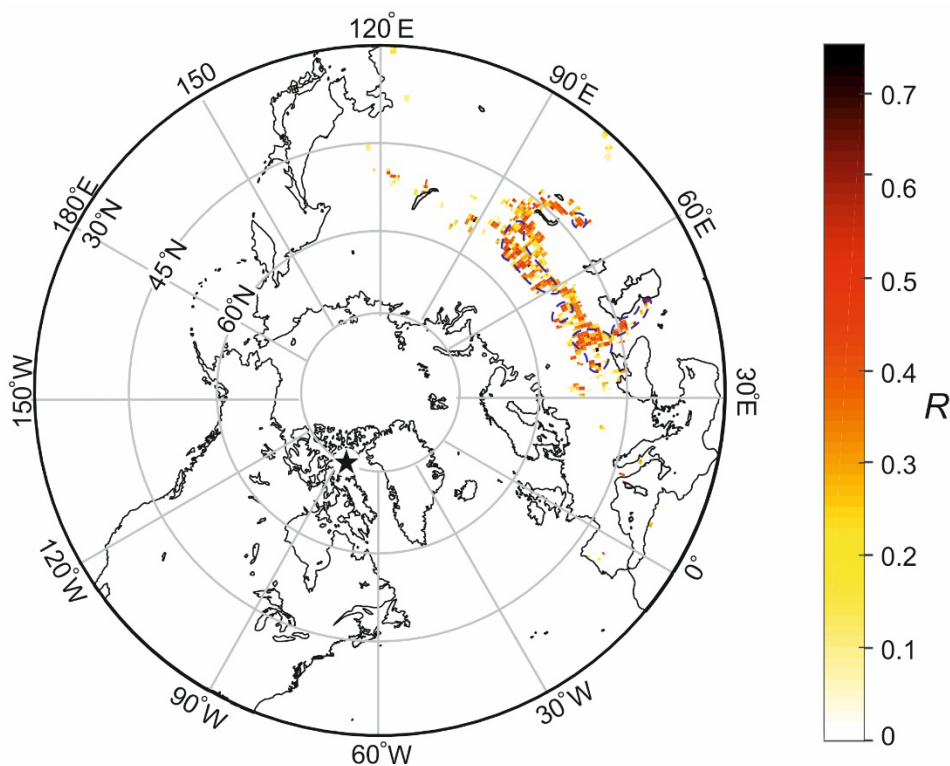
Figure 10: Correlation map of decadal rBC variations in the DV99.1 ice core (coring location shown by star) against reconstructed BC emissions from biomass burning (grassland and forest fires) in the Northern Hemisphere north of 30°N over the period 1900-1990, after Lamarque et al. (2010). Only BC emissions > 0.1 t a⁻¹ per 0.5 x 0.5° map grid cell were considered. Colors indicate the value of Pearson's product-moment correlation coefficient R for each map grid cell. All data were log-transformed prior to computing correlations, an only cells with positive correlations (R > 0) are shown. Blue stippled contours identify areas where correlations are statistically meaningful at the 90 % level of confidence (field significance test; Wilks, 2016; Benjamini and Yekutieli, 2001).